

Research Article

A Comprehensive Model for Circulating Pressure Loss of Deep-water Drilling and Its Application in Liwan Gas Field of China

Yujia Zhai and Zhiming Wang

MOE Key Laboratory of Petroleum Engineering, China University of Petroleum, China

Abstract: Considering the special wellbore configuration and operating environment of deep-water drilling, a comprehensive model for circulating pressure loss of deep-water drilling is established. Based on fluid mechanics theory and heat transfer theory, wellbore temperature and pressure of riser section are calculated and a coupling approach is proposed. Comprehensive factors that affect circulating pressure loss of deep-water drilling are considered in this study. These factors are mud properties, flow regime, drill pipe rotation, drill pipe eccentricity, cuttings bed, tool joints, BHA (Bottom Hole Assembly), drill bit and surface pipeline. The model is applied to Liwan gas field of China. The results show that the data calculated by this model match the field data very well and the model can provide references for designing deep-water drilling hydraulic parameters.

Keywords: Application, circulating pressure loss, deep-water drilling, liwan gas field

INTRODUCTION

With the development of offshore oil and gas resources exploration, the deep-water drilling technology has become a hotspot in recent years. The circulating pressure loss is critical to the analysis of deep-water drilling operations and it can be divided into two parts, which are wellbore pressure loss and additional pressure loss. Wellbore pressure loss represents a significant proportion in circulating pressure loss and the key of calculation is the determination of frictional coefficients and flow regime. Researchers focus on the study of pipe/annular pressure loss very early (Fredrickson and Bird, 1958; Zamora and Lord, 1974) and most of the study were limited to the fluid properties and flow regime (Demirdal and Cunha, 2007; Kelessidis *et al.*, 2011). With the development of the drilling technology, researcher found that variations in annular geometry, drill pipe rotation and eccentricity strongly affect pressure loss during drilling, but most of them were only suited to slimhole well (McCann *et al.*, 1995; Hansen and Sterri, 1995; Ooms and Kampman-Reinhartz, 2000; Ozbayoglu and Sorgun, 2010). Cartalos and Dupuis (1993) noted that the variations in annular clearance such as tool-joint have consequences on the annular pressure loss. Another two studies demonstrated that there is a significant effect of tool-joint on the annular friction pressure loss and the study of Hemphill *et al.* (2007) indicated that the pressure loss increases about 12% of the total annular pressure, while only a small fraction of the length of a tool-joint of drill pipe. The influence of cuttings bed, BHA and

drill bit on pressure loss is relatively small and there are few researches on them in the past, but they could not be ignored when calculating the circulating pressure loss in the condition of deep-water drilling. This study built a new comprehensive model for circulating pressure loss which is appropriate for deep-water drilling. Almost all factors that affect the circulating pressure loss are taken into account. Besides, the variation of wellbore temperature, pressure and temperature coupled and their effects on mud density are considered. Different calculation methods are also adopted to be suitable for different rheological models, flow regimes and boundary conditions. So the accuracy of this model is higher and it can be used in actual engineering. It also will provide theoretical basis for the design of hydraulic parameters in deep-water drilling.

MATHEMATICAL MODELS OF WELLBORE PRESSURE LOSS

According to the fluid mechanic theory, the pressure loss equation in drill pipe can be written as:

$$\Delta p_p = \frac{2f_p \rho_f l v_f^2}{d_{pi}} \quad (1)$$

The annular pressure loss calculating equation is:

$$\Delta p_a = \frac{2f_a \rho_f l v_f^2}{d_{ao} - d_{ai}} \quad (2)$$

The length and size of wellbore and the density and flow velocity of drilling fluid are constant, so the key of calculating wellbore pressure loss is to accurately calculate the coefficient of friction resistance of pipe f_p and of annulus f_a . According to the fluid mechanic theory, coefficient of friction resistance is related to such factors as rheological model, rheological parameter, flow state (laminar or turbulent), Reynolds number and geometric boundary condition.

Drilling fluid rheological model optimization: To choose the right drilling fluid rheological model is the premise of accurately calculating circulating pressure loss. The frequently used drilling fluid rheological models include Power law model, Bingham model, Casson model, Herschel-Buckley model and so on. Different drilling fluid rheological models affect the results to a great extent. So it is necessary to choose the most suitable rheological model before calculating hydraulic parameters.

Fibonacci search method Guo and Wang (2008) is adopted in this study for optimization of drilling fluid rheological models. The method is based on the nonlinear equation regression principle and introduces the function extremum analyse method and optimization solution into fluid rheological model optimization. There is no need to transfer equation when regressing two-parameter equation. It is also easier to regress three-parameter equation and the regression results can achieve optimization in nonlinear equation.

Flow regime identification and friction resistance coefficient selection: Laminar flow and turbulent flow are different in flow mechanism, so selections of friction coefficients are accordingly different. Drilling fluid with different rheological models should adopt different methods to identify flow regimes and calculate friction coefficients, so it is necessary to calculate them, respectively.

Power-law model: The rheological equation of power law fluid is:

$$\tau = k\gamma^n \tag{3}$$

The Reynolds number of power law fluid is:
Pipe flow:

$$Re = \frac{8^{1-n} \rho_f d_{pi}^n v_f^{2-n}}{k \left(\frac{3n+1}{4n}\right)^n} \tag{4}$$

Annular flow:

$$Re = \frac{12^{1-n} \rho_f (d_{ao} - d_{ai})^n v_f^{2-n}}{k \left(\frac{2n+1}{3n}\right)^n} \tag{5}$$

The critical Reynolds number of power law fluid is $Re_c = 3470 - 1370n$. If $Re < Re_c$, it is laminar flow, on the contrary, it is turbulent flow:
Friction coefficients of pipe flow:

$$f_p = 16 / Re \tag{6}$$

Friction coefficients of annular flow:

$$f_a = 24 / Re \tag{7}$$

Use Dodge-Metzner semi-empirical formula when calculate the Friction coefficient of turbulent flow (Dodge and Metzner, 1959):

$$\frac{1}{f_p^{1/2}} = \frac{4}{n^{0.75}} \lg[Re_{M-R} f_p^{(1-0.5n)}] - \frac{0.4}{n^{1.2}} \tag{8}$$

Bingham model: The rheological equation of Bingham fluid is:

$$\tau = \tau_0 + \mu_\infty \gamma \tag{9}$$

Hedstrom and Hanks' methods are adopted to calculate the Renold number, differentiate flow regimes of Bingham fluid (Hanks, 1963). The Reynolds number of Bingham fluid is:
Pipe flow:

$$Re = \frac{\rho_f d_{pi} v_f}{\mu_\infty} \tag{10}$$

The critical Reynolds number of flow regime transformation of Bingham fluid can be calculated using the three equations as follows:

$$Re_c = \frac{He}{8x} \left(1 - \frac{4}{3}x + \frac{1}{3}x^4\right)$$

$$He = \frac{\rho_f \tau_0 d_{pi}^2}{\mu_\infty^2}$$

$$\frac{x}{(1-x)^3} = \frac{He}{16800}$$

Flow regime identification: If $Re < Re_c$, it is laminar flow, on the contrary, it is turbulent flow:
Friction coefficient of laminar flow:

$$\frac{f_p}{16} = \frac{1}{\text{Re}} + \frac{\text{He}}{6\text{Re}^2} + \frac{\text{He}^2}{3f_p \text{Re}^8} \quad (11)$$

Friction coefficient of turbulent flow:

$$f_p = \frac{0.053}{(3.2\text{Re})^{0.2}} \quad (12)$$

Replace pipe diameter d_i with annular equivalent diameter $d_{ao}-d_{ai}$ to calculate annular flow.

Casson model: The rheological equation of Casson fluid is:

$$\tau^2 = C_c + \mu_c^2 \gamma^2 \quad (13)$$

The Reynolds number of Casson fluid is:
Pipe flow:

$$\text{Re} = \frac{\rho_f d_{pi} v_f}{\mu_c \left[\left(1 - \frac{C_c^2 d_{pi}}{294 \mu_c v_f}\right)^{\frac{1}{2}} + \frac{C_c}{7} \left(\frac{8 d_{pi}}{\mu_c v_f}\right)^{\frac{1}{2}} \right]^2} \quad (14)$$

Annular flow:

$$\text{Re} = \frac{\rho_f (d_{ao} - d_{ai}) v_f}{\mu_c \left[\left(1 - \frac{C_c^2 (d_{ao} - d_{ai})}{200 \mu_c v_f}\right)^{\frac{1}{2}} + \frac{C_c}{5} \left(\frac{3(d_{ao} - d_{ai})}{\mu_c v_f}\right)^{\frac{1}{2}} \right]^2} \quad (15)$$

The critical Reynolds numbers of flow regime transformation of Casson fluid is $\text{Re}_c = 2100$. If $\text{Re} < \text{Re}_c$, it is laminar flow, on the contrary, it is turbulent flow.

Friction resistance coefficient of laminar flow is the same with that of the power law fluid. Nikuradse equation is used to calculate friction coefficient of turbulent flow:

$$\frac{1}{f_p^{1/2}} = 4 \lg[\text{Re} f_p^{1/2}] - 0.395 \quad (16)$$

Herschel-Buckley model: The rheological equation of Herschel-Buckley fluid is:

$$\tau = \tau_0 + k \gamma^n \quad (17)$$

The Reynolds number of Herschel-Buckley fluid is:
Pipe flow:

$$\text{Re} = \frac{8^{1-n} \rho_f d_{pi}^n v_f^{2-n}}{k \left(\frac{3n+1}{4n}\right)^n \left[1 + \frac{3n+1}{2n+1} \left(\frac{n}{6n+2}\right)^n \left(\frac{d_{pi}}{v_f}\right)^n \frac{\tau_0}{k}\right]} \quad (18)$$

Annular flow:

$$\text{Re} = \frac{12^{1-n} \rho_f (d_{ao} - d_{ai})^n v_f^{2-n}}{k \left(\frac{2n+1}{3n}\right)^n \left[1 + \frac{(2n+1)^{1-n}}{n+1} \left(\frac{n}{4}\right)^n \left(\frac{d_{ao} - d_{ai}}{v_f}\right)^n \frac{\tau_0}{k}\right]} \quad (19)$$

The critical Reynolds number of Herschel-Buckley fluid is $\text{Re}_c = 3470-1370n$. $\text{Re} < \text{Re}_c$, it is laminar flow, on the contrary, it is turbulent flow.

Friction resistance coefficient of laminar flow is the same with that of power law. Torrance equation is used to calculate the friction coefficient of turbulent flow here:

$$\frac{1}{f_p^{1/2}} = \frac{2.69}{n} - 2.95 + \frac{4.53}{n} \lg[\text{Re} f_p^{(1-0.5n)}] + \frac{4.53}{n} \lg\left(1 - \frac{\tau_0}{\tau_w}\right) \quad (20)$$

MATHEMATICAL MODELS OF TEMPERATURE FIELD

Basic hypothesis: The following assumptions are made in the formulation of the model (Fig. 1):

- The fluid is incompressible and the flow in the wellbore is one-dimensional
- The condition of gas cut and circulation loss are not considered
- Considering the heat transfer in formation and seawater but the convection and heat source are not taken into account
- The state of heat transfer in wellbore is steady but it is unsteady in formation
- The heat conduction of wellbore and its surrounding formation/seawater occur only in the radial direction
- The formation is radially symmetrical and infinite
- The temperature distribution of seawater stay the same during drilling process

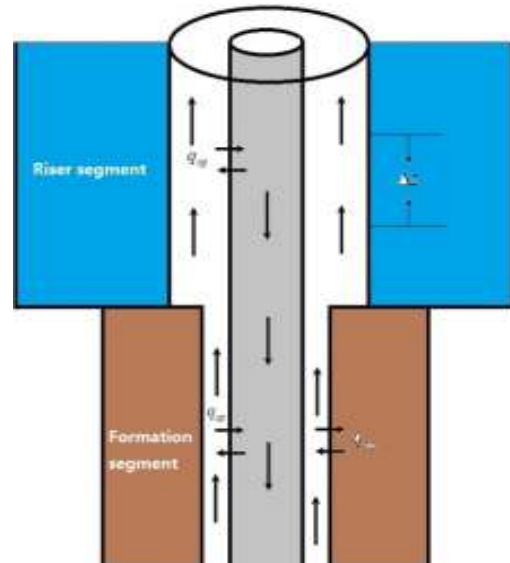


Fig. 1: The model of wellbore flow and heat transfer

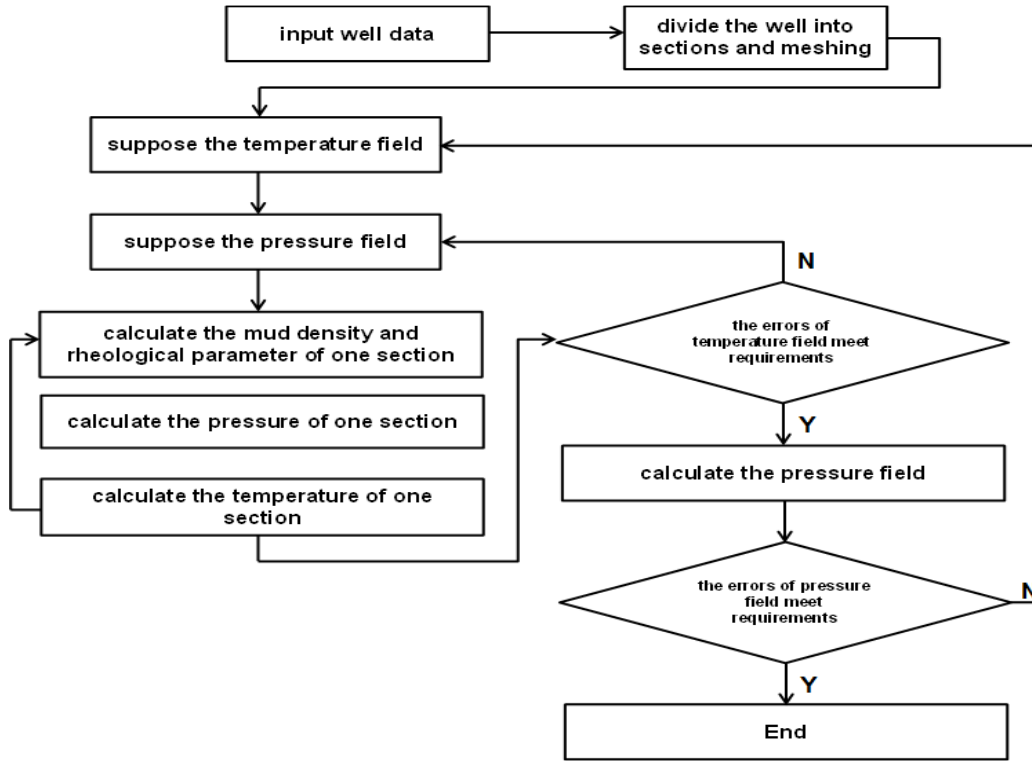


Fig. 2: The flow chart of temperature-pressure coupling

- During the circulation, the specific heat capacity and thermal conductivity of formation/seawater, drill pipe and casing remain unchanged

Heat transfer model:

During drilling: Temperature field equation in drill pipe (Wang *et al.*, 2010a):

$$\rho_f C_f \frac{\pi}{4} d_{pi}^2 \frac{\partial T_p}{\partial t} = -\rho_f C_f Q_f \frac{\partial T_p}{\partial z} + q_{ap} + q_p \quad (21)$$

Annular temperature field equation:

$$\rho_f C_f \frac{\pi}{4} (d_{ai}^2 - d_{po}^2) \frac{\partial T_a}{\partial t} = \rho_f C_f Q_f \frac{\partial T_a}{\partial z} + q_{ea} - q_{ap} + q_a \quad (22)$$

where,

$$q_{ea} = \begin{cases} \frac{(T_{sea} - T_a)}{\left(\frac{f(t)}{2\pi k_{sea}} + \frac{1}{\pi d_{ri} h_{ri}} \right)} & \text{(sea segment)} \\ \frac{(T_e - T_a)}{\left(\frac{f(t)}{2\pi k_e} + \frac{1}{\pi d_{ai} h_{ai}} \right)} & \text{(formation segment)} \end{cases}$$

$$q_{ap} = \frac{(T_a - T_p)}{\left(\frac{1}{\pi d_{po} h_{po}} + \frac{1}{\pi d_{pi} h_{pi}} \right)}$$

Stop drilling: Temperature field equation in drill pipe:

$$\rho_f C_f \frac{\pi D_{pi}^2}{4} \frac{\partial T_p}{\partial t} = \frac{2\pi k_w}{\ln \frac{d_{po}}{d_{pi}}} (T_a - T_p) \quad (23)$$

Annular temperature field equation:

$$\rho_f C_f \pi \frac{d_{ai}^2 - d_{po}^2}{4} \frac{\partial T_a}{\partial t} = \frac{(T_e - T_a)}{\frac{f(t)}{2\pi k_e} + \frac{d_{ai}}{2\pi k_w}} - \frac{2\pi k_w}{\ln \frac{d_{po}}{d_{pi}}} (T_a - T_p) \quad (24)$$

Wellbore temperature-pressure coupling: The flow chart of temperature-pressure coupling is presented in Fig. 2. Using computer program to solve the problem, we got the drilling fluid density and effect viscosity distribution along the wellbore which considered the effect of temperature and pressure.

Model solution:

Initial condition: For whole wellbore, assuming that the initial temperature of drilling fluid in casing and annulus are equal to the sea temperature and geothermal temperature of undisturbed, that can be expressed by:

- Sea section: $T_p(z, t = 0) = T_a(z, t = 0) = T_{sea}(z)$

- Formation section: $T_p(z, t = 0) = T_a(z, t = 0) = T_e(z)$

Boundary conditions: The inlet temperature can be directly measured, so the boundary condition is $T(z, t = 0) = T_{in}$. The drilling fluid temperature at bottom hole satisfied $T_a(z = H, t) = T_p(z = H, t) - \Delta T_{bit}$, where, ΔT_{bit} is the temperature drop through the drill bit. The geothermal temperature at a certain distance from the formation or sea section is equal to that of undisturbed:

$$T_e(z = H + \Delta z, t) = T_e(H + \Delta z)$$

$$T_{sea}(z = H + \Delta z, t) = T_{sea}(H + \Delta z)$$

Discrete solution: Because the model is complex, analytic solution does not apply to solve the equations and the numerical method is adopted here. Considering the stability of differential equations, fully implicit method is used here to disperse the equations. In these equations, first time derivatives are dispersed by using backward difference method while first space derivatives are dispersed by one-order upwind difference method. Second space derivatives are dispersed by central difference scheme, the differential equations can be written as:

During drilling: Difference scheme in drill pipe:

$$\rho_f C_f \frac{\pi d_{pi}^2}{4} \frac{T_{p,i}^{j+1} - T_{p,i}^j}{\Delta t} = -\rho_f C_f Q_f \frac{T_{p,i}^{j+1} - T_{p,i}^j}{\Delta z} + q_{ap} + q_p \quad (25)$$

Difference scheme in annulus:

$$\rho_f C_f \frac{\pi}{4} (d_{ai}^2 - d_{po}^2) \frac{T_{a,i}^{j+1} - T_{a,i}^j}{\Delta t} = \rho_f C_f Q_f \frac{T_{a,i}^{j+1} - T_{a,i}^j}{\Delta z} + q_{ea} - q_{ap} + q_a \quad (26)$$

Stop drilling: Difference scheme in drill pipe:

$$\rho_f C_f \frac{\pi D_{pi}^2}{4} \frac{T_{p,i}^{j+1} - T_{p,i}^j}{\Delta t} = \frac{2\pi k_w}{\ln \frac{d_{po}}{d_{pi}}} (T_a - T_p) \quad (27)$$

Difference scheme in annulus:

$$\rho_f C_f \frac{\pi}{4} \frac{d_{ai}^2 - d_{po}^2}{\Delta t} \frac{T_{a,i}^{j+1} - T_{a,i}^j}{\Delta t} = \frac{2\pi k_w}{\frac{f(t)}{2\pi k_e} + \frac{\ln \frac{d_{po}}{d_{pi}}}{2\pi k_w}} - \frac{2\pi k_w}{\ln \frac{d_{po}}{d_{pi}}} (T_a - T_p) \quad (28)$$

MATHEMATICAL MODELS OF ADDITIONAL PRESSURE LOSS

Additional pressure loss of eccentricity and drill pipe rotation: To calculate circulating loss more accurately, the effects of drill pipe eccentricity and rotation must be considered.

The influence coefficient of drill pipe eccentricity is as follows (Haciislamoglu and Cartalos, 1994):

Laminar flow:

$$c_{ec} = 1 - 0.072 \bar{e} \left(\frac{d_{po}}{d_w} \right)^{0.8454} - 1.5 e^{-2} \sqrt{n} \left(\frac{d_{po}}{d_w} \right)^{0.1852} + 0.96 e^{-3} \sqrt{n} \left(\frac{d_{po}}{d_w} \right)^{0.2527} \quad (29)$$

Turbulent flow:

$$c_{ec} = 1 - 0.048 \bar{e} \left(\frac{d_{po}}{d_w} \right)^{0.8454} - \frac{2}{3} e^{-2} \sqrt{n} \left(\frac{d_{po}}{d_w} \right)^{0.1852} + 0.285 e^{-3} \sqrt{n} \left(\frac{d_{po}}{d_w} \right)^{0.2527} \quad (30)$$

The influence coefficient of drill pipe rotation is as follows (Cartalos and Dupuis, 1993):

$$c_r = \sqrt{1 + 1.5 e_{max}^2} \quad (31)$$

When the sine bending and cosine bending of drill pipe occur, \bar{e} is the average eccentricity of bending annulus while e_{max} is the maximum eccentricity of curvature annulus:

$$e_{max} = \frac{d_w - d_c}{d_w - d_{po}} \quad (32)$$

$$\bar{e} = \sqrt{\frac{2}{3} \left(\sqrt{\frac{3}{2} e_{max} + 1} - 1 \right)} \quad (33)$$

where, d_c is the diameter of stabilizer or external upset tool joint.

Additional pressure loss of tool joints: Tool joints have a great effect on circulating pressure loss, especially in drill pipe. Because of the great vertical depth of the deep-water wells the effect of tool joints must be considered. Otherwise errors will be generated. Previous studies show that additional pressure loss caused by tool joints account for 10 to 20% of pressure loss in pipes (Wang, 2008). The schematic diagram is shown in Fig. 3. According to fluid mechanic theory,

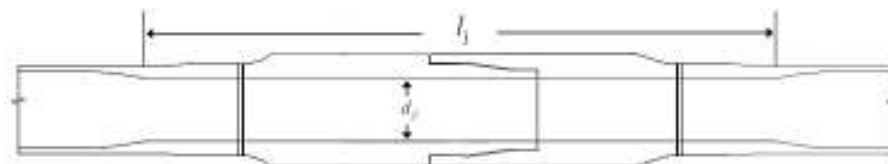


Fig. 3: The outline of tool joint

the influence coefficient of tool joints is deduced as follows:

$$c_j = \frac{l_p}{l_p + l_j} + \frac{l_j}{l_p + l_j} \left(\frac{d_{pi}}{d_{ji}} \right)^{4.8} \quad (34)$$

where,

- l_p : The length of single drill pipe
- l_j : The length of tool joint
- d_{pi} : The inner diameter of drill pipe
- d_{ji} : The inner diameter of tool joint

Because of the large annular clearance, the low annular velocity of deep-water wells and the low ratio of annular pressure loss to circulating pressure loss in general conditions, the effect of tool joints on annular pressure loss is not considered.

Additional pressure loss of cuttings bed: Researches show that because the highly-deviated section is long, the cuttings are easy to form cuttings bed in the annular bottom and the effect of cuttings bed on annular pressure loss increases as the highly-deviated section grows (Wang *et al.*, 2010b; Wang *et al.*, 2011). Suppose that annulus achieves stable and cuttings bed of certain height exist, consider the axial velocity difference between solid-liquid phases in suspension layer and not consider the slide of cuttings bed and gravity pressure drop, the followings are deduced according to fluid mechanic theory:

$$\Delta p_{cb} = \frac{((1-C_s)f_{fw}\rho_f v_f^2 S_{hw} + C_s f_{sw}\rho_s v_s^2 S_{hw} + f_{hcb}\rho_f v_f^2 S_{hcb})}{2A_n} \quad (35)$$

Additional pressure loss of BHA: Currently when hydraulic parameters are designed and calculated, the pressure loss of BHA are usually neglected or set as a certain value by experience. This can meet the requirements of engineering projects in drilling vertical, shallow-directional and horizontal wells. But it is unreasonable in drilling extended reach well especially in deep-water drilling.

According to the working features of BHA, the following methods can be adopted to calculate its pressure loss.

Use constant: This method is simple and convenient. It can be used when the pressure loss of BHA is low and the drilling parameters are small.

Use working parameter tables: Users provide the parameter table of the BHA, including displacement, pressure drop, revolution and power. Based on the actual displacement, the interpolation method is used and then the actual pressure loss is calculated:

$$\Delta p_m = \Delta p_1 + \frac{\Delta p_2 - \Delta p_1}{Q_2^2 - Q_1^2} (Q_a^2 - Q_1^2) \quad (Q_1 < Q_a < Q_2) \quad (36)$$

Table 1: Operational parameters of 311 mm (12-1/4'') segment

Flow rate, L/s	55-60
ROP, m/h	10-60
RPM, r/min	100-150
ρ_f , g/cm ³	1.10-1.16
ρ_s , g/cm ³	2.60
u , mPa.s	25
d_s , mm	5

where,

- Δp_m : The pressure loss of BHA
- Q_a : The actual annular displacement

Use actual data to calculate pressure loss coefficient:

When the drilling is stable and the hole cleaning condition is known, with the use of the following relation, the pressure loss coefficient of BHA is calculated. Then the calculated coefficient is used to calculate the pressure loss of the following sections. This method can meet the requirements of projects when the drilling parameters change slightly:

$$\Delta p_m = \Delta p_c - \Delta p_s - \Delta p_p - \Delta p_b - \Delta p_a \Rightarrow c_m = \Delta p_m / Q_a^2 \quad (37)$$

Additional pressure loss of drill bit and surface pipeline:

Bit pressure loss calculating method is the same with the conventional one and it can be expressed as:

$$\Delta p_b = \frac{0.5 \rho Q_a^2}{c_n^2 A_o^2} \quad (38)$$

where,

- c_n : Flow coefficient of the nozzle
- A_o : The total area of nozzles

The surface pipeline can also be seen as the drill string. Replace the inner diameter of drill pipe with that of surface pipeline, we can get the surface pipeline pressure loss.

THE MODEL FOR CIRCULATING PRESSURE LOSS OF DEEPWATER DRILLING

The operation conditions are very different along the wellbore in deep-water drilling. So the pressure loss of dill pipe and annulus are calculated by sectioning method. The influence of eccentricity, rotation, tool joints and cuttings bed on pressure loss are relatively small and they must be handled as a whole, therefore, they are seen as constant in this study. To sum up, the calculating equation of circulating pressure loss is:

$$\Delta p_c = \sum c_{eci} c_{ri} \Delta p_{ai} + \sum c_{ji} \Delta p_{pi} + \Delta p_{cb} + \Delta p_m + \Delta p_b + \Delta p_{sp} \quad (39)$$

RESULTS AND DISCUSSION

The study takes a well in Liwan gas field as an example to verify the accuracy of the model. Operational parameters, characteristics of drilling fluid

Table 2: Calculated results of different depths of 311 mm (12-1/4'') segment

Depth, m	Conventionality, MPa	Tool joint, MPa	Cuttings bed, MPa	Rotation, MPa	Eccentricity, MPa	Combination, MPa	Measured value, MPa
2190	17.037	18.065	/	17.055	16.996	18.044	18.145
2550	17.781	18.919	/	17.815	17.703	18.919	18.933
2850	17.353	18.916	19.051	17.386	17.278	19.645	19.815
3210	18.965	20.521	/	19.023	18.828	20.520	20.532
3540	18.155	20.106	19.388	18.205	18.039	21.323	21.543
3870	18.856	20.968	20.312	18.925	18.697	22.130	21.922
4200	21.723	22.933	/	21.808	21.543	22.937	22.951

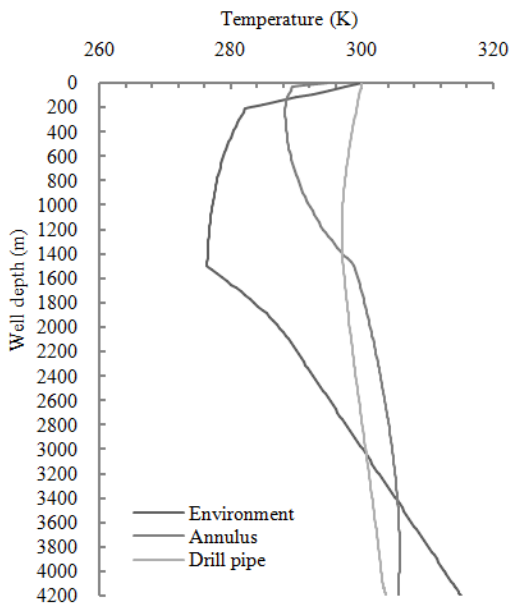


Fig. 4: Wellbore temperature distribution in the drilling process

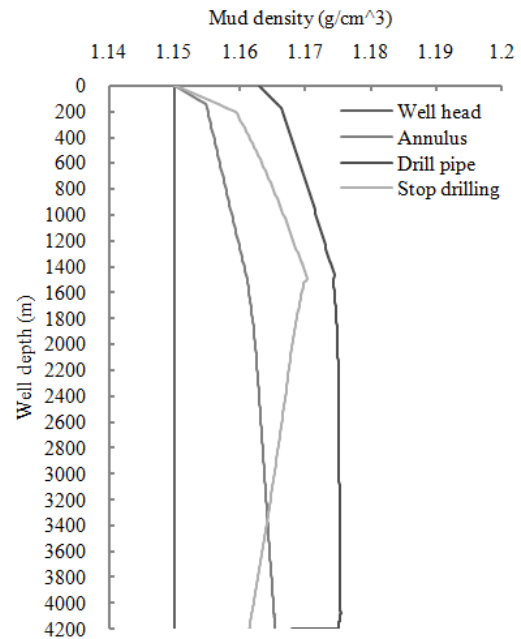


Fig. 5: Density distribution of drilling fluid

and cuttings are listed in Table 1 and the result is shown in Table 2.

Interaction between temperature, pressure and drilling fluid rheology: Figure 4 shows the curves of mud temperature vary with well depth along the wellbore. The studies found that circulating time has a great influence on temperature profile. With the increasing of circulating time, the temperature changed more and more slightly and after 16 h, we can assume that the temperature stops changing. The turning point on each curve is the position of mudline. In drill pipe, the mud temperature drops slowly from wellhead to the mudline and it changes slightly below the mudline. The highest mud temperature appears in the annulus above the bottom hole instead of in the bottom hole. This is because the high temperature of formation makes the mud temperature increase and that the heat conducts to the above segment.

Figure 5 illustrates that temperature and pressure have a big influence on mud density in deep-water drilling. With the decreasing of temperature and the rising of pressure along with well depth in riser segment, the mud density increases gradually from well

head to the mudline. But below the mudline, the mud density changes slightly in the drilling process. When circulating stops, the mud temperature in annulus and drill pipe is the same and the mud density declines sharply along with the well depth. As is known, the higher temperature will cause the lower density while the higher pressure will cause the higher density, thus under these two circumstances, the mud density will be changed. From the mudline to the bottom of hole, the temperature and pressure increase simultaneously. So it is clear that the effect of temperature on mud density is bigger than that of pressure.

The experimental result indicates that increasing temperature leads to effective viscosity decreasing while pressure has the opposite effect. At low temperatures, pressure plays a leading role in changing mud viscosity. With the rising of temperature, the effective viscosity decreases rapidly. Meanwhile the effect of pressure on it weakens. As is shown in Fig. 6, the effective viscosity changes little along the wellbore in riser segment when the effect of temperature and pressure are not taken into account. This trend will be very different when these two factors are considered.

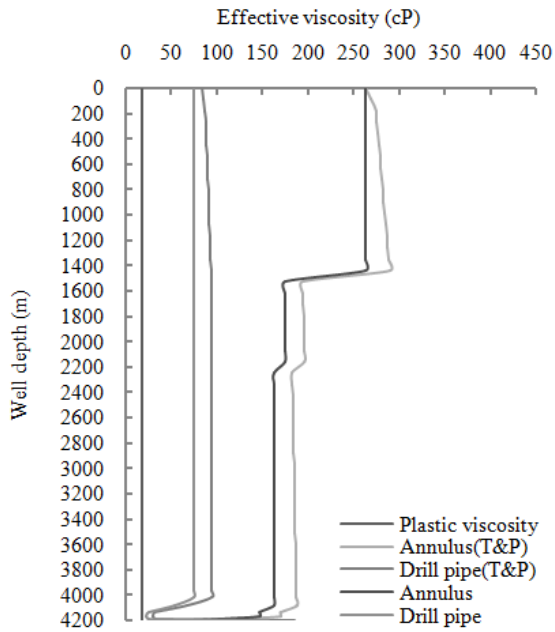


Fig. 6: Effective viscosity distribution of drilling fluid

Figure 6 manifests that the effective viscosity increases with the increasing of well depth in annulus above the mudline and this increase is relatively small in drill pipe. Below the mudline, the variation of mud viscosity is very little, which is because the synergistic effect of temperature and pressure makes the changing counteract. The effective viscosity in drill pipe and in annulus is bigger when the effect of temperature and pressure are considered.

Circulating pressure loss sensitivity analysis:

The calculation of circulating loss: Using the models proposed above, the calculated results are got and shown in Table 2. “Conventionality” means that none of the factors are considered, “combination” means taking all these factors into account and “measured” means the field data. “Tool joint” means only considering the effect of tool joint and the rest items mean the same way as “tool joint” does.

The results show that the conventional methods lead to a relatively smaller calculation result and the maximum error can reach about 3 MPa. The tool joints and the cuttings bed have the greatest influence on

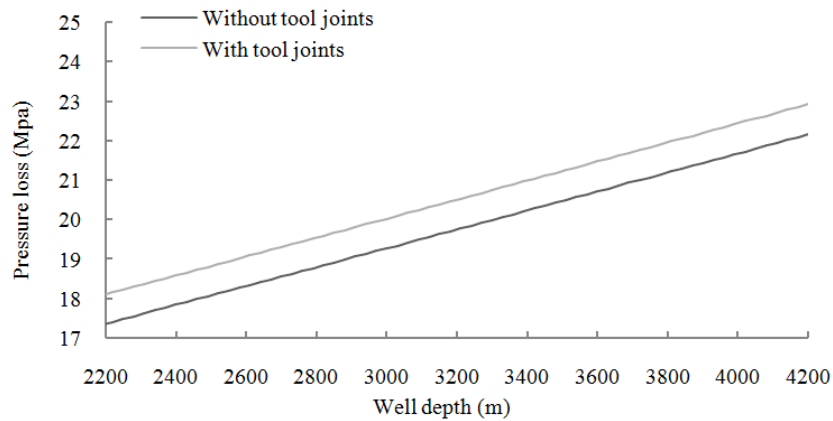


Fig. 7: The influence of tool joints on pressure loss

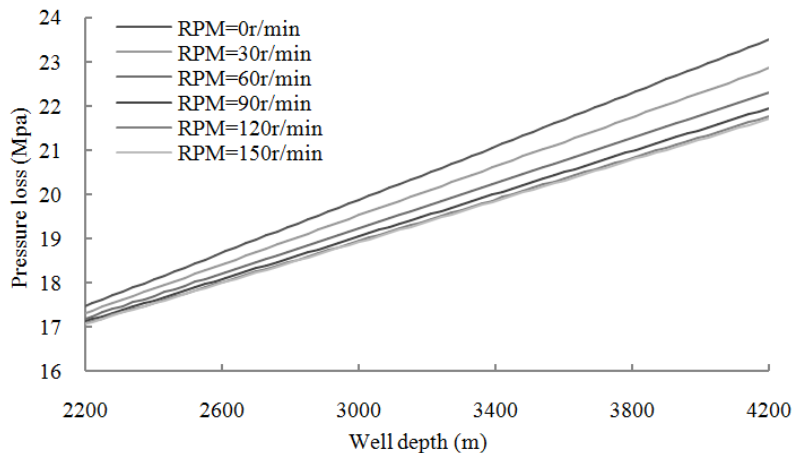


Fig. 8: The influence of drill pipe rotation speed on pressure loss

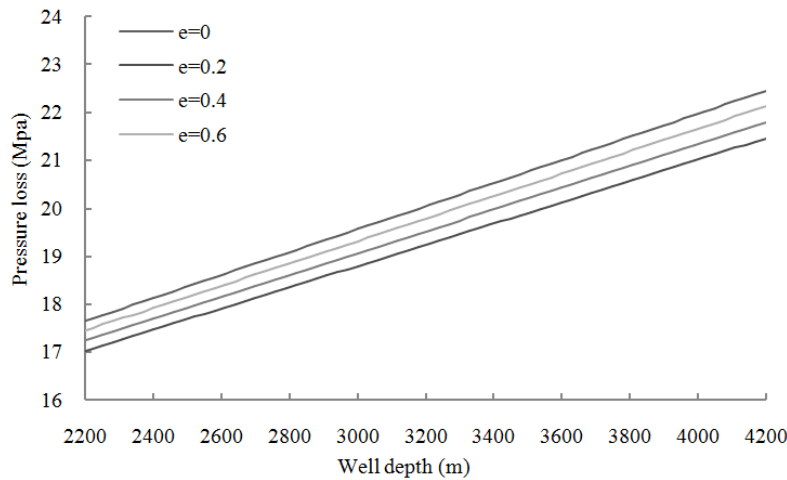


Fig. 9: The influence of eccentricity on pressure loss

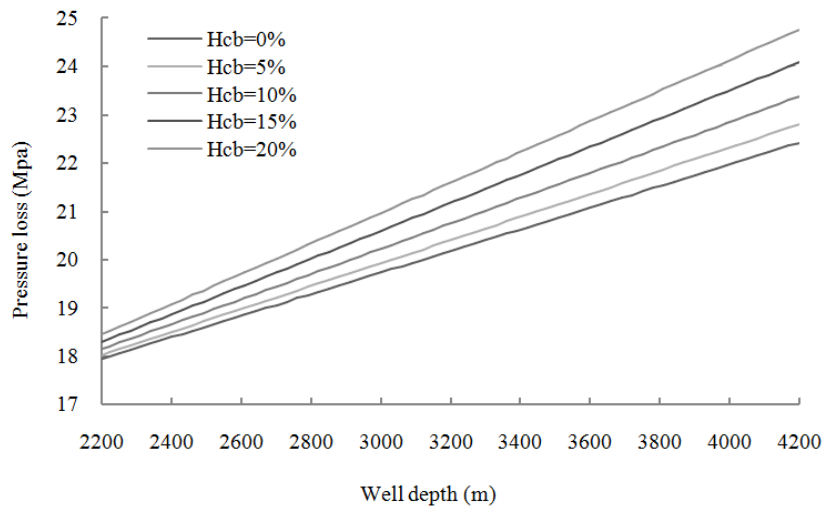


Fig. 10: The influence of cuttings bed on pressure loss

circulating pressure loss while the influence of eccentricity and rotation is relatively small. Among these factors, tool joints, cuttings bed and drill pipe rotation lead the calculation value bigger. Tool joint can make circulating pressure loss increase by 2.1 MPa while drill pipe rotation only makes it increase by 0.085 Mpa. The factor of eccentricity is very different from the above. It can make the value smaller than the conventional result and the difference between them can reach 0.16 MPa. The combination value considers all these factors and thus simulation and calculation are more close to the situation. The calculation error is reduced from 15.73% down to 1.02%.

Sensitivity of pressure loss to tool joints: As expected, additional pressure loss is observed with the presence of the tool joints. Figure 7 shows the pressure loss curves for drill pipe with and without tool joints. The presence of tool joints significantly increases the

pressure loss and this effect has little relation to the well depth. The average value increases about 0.76 MPa at different depth.

Sensitivity of pressure loss to drill pipe rotation: Pressure loss in highly-deviated and horizontal well section is particularly sensitive to drill pipe rotation. Figure 8 shows the effect of drill pipe rotation speed on pressure loss. With the increase of well depth, the pressure loss increases linearly at different rotation speeds. Increasing rotation speed can make the pressure loss decrease, which is because cuttings can remain a suspending state when rotation speed reaches a certain value and cuttings bed cannot form in annulus. The rotation speed ranges from 0 to 150 rpm under this condition. When drill pipe is static, the pressure loss in bottom hole can be 24.55 MPa. With the increase of rotation speed (less than 60 rpm), the pressure loss drops dramatically and it can decrease by 23.4 MPa in

the same spot. The effect of drill pipe rotation weakens as the speed increases and this trend is especially obvious when the rotation speed passes 60 rpm. One hundred and twenty rpm is a critical point in this case. The pressure loss will change little when the value is beyond this point.

Sensitivity of pressure loss to drill pipe eccentricity:

In highly-deviated and horizontal well section, rotating drill pipe do not remain concentric. And the variation of drill pipe position can lead to a different flow velocity between upper annulus and lower annulus. Because the flowing space becomes small, the drilling fluid flows faster in lower annulus and cuttings will be much easier to be carried. When the cuttings concentration is not too high, the cuttings bed will not form in the lower annulus. This is the reason why concentricity can make the pressure loss decrease. The result that pressure loss reduces with the increasing eccentricity is the same as reported in literature. Figure 9 shows that a small eccentricity can lead to a great drop in pressure loss and the maximum value decreases by nearly 1 Mpa. With the increase of eccentricity, the pressure loss increases gradually. When the eccentricity is bigger than 0.8, the pressure loss exceeds the conventional value. That is because the large eccentricity makes the gap too small to let the cuttings go through and the cuttings bed forms finally. The behaviour is observed for all geometries.

Sensitivity of pressure loss to cuttings bed:

The formation of cuttings bed is very common in deep-water drilling. Because of such formation, the shape of annulus changes and the annular gap becomes smaller while the friction coefficient becomes larger. Figure 10 shows that the influence of cuttings bed on pressure loss is obvious. With the increase of cuttings bed height, the pressure loss increases, the influence of cuttings bed on pressure loss becomes greater as the well depth increases.

CONCLUSION AND RECOMMENDATIONS

Conclusion:

- On the basis of studies and analysis, a calculation method of friction coefficient which is suitable for deep-water drilling is presented. The influence coefficient of tool joints, eccentricity, rotation and cuttings bed are given in this study.
- Based on the traditional circulating pressure loss calculating model, considered the particularity of the deep-water wells, a model for calculating the circulating pressure loss in deep-water drilling is developed. The model is of high precision and can be applied to the actual engineering.

- The tool joints and the cuttings bed have the greatest influence on circulating pressure loss while the influence of eccentricity and rotation is relatively small. So the effect of tool joints and cuttings bed must be considered when drilling. Most factors can make the circulating pressure loss increase while drill pipe rotation makes it decrease.

Recommendations:

- As the gas cut, leakage and other complex situations are not considered in this study, the model only applies to the normal drilling state. Therefore, it is recommended that a new and more common model on circulating pressure loss could be proposed.
- The model is only validated by field data and it can be tested when more experimental data are available. In this case, we can determine the application range of the model more accurately.

ACKNOWLEDGMENT

This study was supported by Basic Research on Drilling and Completion of Critical Wells for Oil and Gas (Grant No. 51221003) and the State Science and Technology Major Project (Large Oil and Gas Fields and Coal Bed Methane Development, Grant No.: 2011ZX05009-005). The authors wish to thank CNOOC Research Institute for collecting and providing field data for the verification of this new model.

NOMENCLATURE

- A_0 : Total area of nozzles, m^2
- A_h : Cross section area of suspended layer, m^2
- c : Influence coefficient, dimensionless
- c_n : Flow coefficient of the nozzle, dimensionless
- C_c : Casson C value, $Pa^{0.5}$
- C_f : Specific heat capacity, $J/(kg \cdot K)$
- C_s : Cuttings volume concentration, %
- d : Diameter, m
- f : Friction coefficient, dimensionless
- $f(t)$: Time function, dimensionless
- h : Convective transfer coefficient, $w/(m^2 \cdot K)$
- H : Height, m
- He : Hedstrom number, dimensionless
- k : Heat conductivity coefficient, $w/(m \cdot K)$
- l : Length, m
- ΔP_c : Circulating pressure loss, Pa
- ΔP_p : Pressure loss in drillpipe, Pa
- q : Frictional heating, w
- q_{ap} : Heat exchange between annulus and drillpipe, w
- q_{ea} : Heat exchange between formation and annulus, w
- Q_a : Actual annular displacement, m^3/s
- Q_f : Mass flow rate, Kg/s

Re : Reynolds number, dimensionless
 Re_c : Critical Reynolds number, dimensionless
 S : Wetted perimeter, m
 T : Temperature, K
 v_f : Flow velocity, m/s

Greeks:

ρ_f : Drilling fluid density, kg/m³
 τ : Shear stress, Pa
 τ_0 : Yield value, Pa
 τ_w : Wall shear stress, Pa
 k : Consistency coefficient, Pa·sⁿ
 γ : Shear rate, s⁻¹
 n : Flow behavior index, dimensionless
 μ_∞ : Plastic viscosity, Pa·s
 μ_c : Casson plastic viscosity, Pa·s

Subscripts:

p : Drillpipe
 a : Annulus
 m : BHA
 b : Drill bit
 cb : Cuttings bed
 sp : Surface pipelines
 j : Tool joint
 i : Inner
 o : Outer
 c : Stabilizer or external upset tool joint
 sea : Sea water
 e : Formation
 in : Inlet
 ec : Drillpipe eccentricity
 r : Drillpipe rotation
 w : Wellbore wall
 h : Suspended layer

REFERENCES

- Cartalos, U. and D. Dupuis, 1993. An analysis accounting for the combined effect of drillstring rotation and eccentricity on pressure losses in slimhole drilling. Proceeding of SPE/IADC Drilling Conference. Amsterdam, Netherlands, Feb. 23-25.
- Demirdal, B. and J.C. Cunha, 2007. Pressure losses of non-Newtonian fluids in drilling operations. Proceeding of International Oil Conference and Exhibition. Veracruz, Mexico, June 27-30.
- Dodge, D.W. and A.B. Metzner, 1959. Turbulent flow of non-Newtonian systems. AIChE J., 5(2): 189-204.
- Fredrickson, A.G. and R.B. Bird, 1958. Flow of non-Newtonian fluid in annuli. Ind. Eng. Chem., 50: 347.
- Guo, X.L. and Z.M. Wang, 2008. Precise method of calculating circulating pressure loss in extended reach wells. J. Oil Gas Technol., 30(5): 99-102.
- Haciislamoglu, M. and U. Cartalos, 1994. Practical pressure loss predictions in realistic annular. Proceeding of the SPE 69th Annual Technical Conference and Exhibition. New Orleans, U.S.A., pp: 25-28.
- Hanks, R.W., 1963. The laminar-turbulent transition for fluids with a yield stress. AIChE J., 9(3): 306-309.
- Hansen, S.A. and N. Sterri, 1995. Drill pipe rotation effects on frictional pressure losses in slim annuli. Proceeding of the SPE Annular Conference and Exhibition. Dallas, U.S.A., pp: 22-25
- Hemphill, T., P. Bern, J.C. Rojas and K. Ravi, 2007. Field validation of drillpipe rotation effects on equivalent circulating density. Proceeding of the SPE Annual Technical Conference and Exhibition. Anaheim, U.S.A., pp: 11-14.
- Kelessidis, V.C., P. Dalamarinis and R. Maglione, 2011. Experimental study and predictions of pressure losses of fluids modelled as Herschek-Bulkley in concentric and eccentric annuli in laminar, transitional and turbulent flows. J. Petrol. Sci. Eng., 77: 305-312.
- McCann, R.C., M.S. Quigley, M. Zamora and K.S. Slater, 1995. Effect of high-speed pipe rotation on pressure in narrow annuli. SPE Drill. Completion, 10(2): 96-103.
- Ooms, G. and B.E. Kampman-Reinhartz, 2000. Influence of drillpipe rotation and eccentricity on pressure drop over borehole with Newtonian liquid during drilling. SPE Drill. Completion, 15(4): 249-253.
- Ozbayoglu, E.M. and M. Sorgun, 2010. Frictional pressure loss estimation of non-Newtonian fluids in realistic annulus with pipe rotation. J. Can. Petrol. Technol., 49(12): 57-64.
- Wang, Z.M., 2008. Fluid Mechanics in Petroleum Engineering. Petroleum Industry Press, Beijing, pp: 31.
- Wang, Z.M., X.M. Hao and X.L. Guo, 2011. A study on the thickness of a cutting bed monitor and control in an extended reach well. Petrol. Sci. Technol., 29(13): 1397-1406.
- Wang, Z.M., X.N. Hao and X.Q. Wang, 2010a. Numerical simulation on deepwater drilling wellbore temperature and pressure distribution. Petrol. Sci. Technol., 28: 911-919.
- Wang, Z.M., Y.J. Zhai and X.N. Hao, 2010b. Numerical simulation on three layer dynamic cutting transport model and its application on extended well drilling. Proceeding of the IADC/SPE Asia Pacific Drilling Technology Conference and Exhibition. Ho Chi Minh City, Vietnam, pp: 1-3.
- Zamora, M. and D.L. Lord, 1974. Practical analysis of drilling mud flow in pipes and annuli. Proceeding of the 49th Annual Fall Meeting of Society of Petroleum Engineers of AIME. Houston, Texas, October 6-9.